

The In-Gap Electronic State Spectrum of Methylammonium Lead Iodide Single-Crystal Perovskites

Valerio Adinolfi, Mingjian Yuan, Riccardo Comin, Emmanuel S. Thibau, Dong Shi, Makhsud Saidaminov, Pongsakorn Kanjanaboos, Damir Kopilovic, Sjoerd Hoogland, Zheng-Hong Lu, Osman M. Bakr, and Edward H. Sargent

Version Post-Print/Accepted Manuscript

Citation (published version) Adinolfi, V., Yuan, M., Comin, R., Thibau, E., Shi, D., & Saidaminov, M. et al. (2016). The In-Gap Electronic State Spectrum of Methylammonium Lead Iodide Single-Crystal Perovskites. *Advanced Materials*, 28(17), 3406-3410. <http://dx.doi.org/10.1002/adma.201505162>

Publisher's Statement This is the peer reviewed version of the following article: Adinolfi, V., Yuan, M., Comin, R., Thibau, E., Shi, D., & Saidaminov, M. et al. (2016). The In-Gap Electronic State Spectrum of Methylammonium Lead Iodide Single-Crystal Perovskites. *Advanced Materials*, 28(17), 3406-3410, which has been published in final form at <http://dx.doi.org/10.1002/adma.201505162>. This article may be used for non-commercial purposes in accordance with Wiley Terms and Conditions for Self-Archiving.

How to cite TSpace items

Always cite the **published version**, so the author(s) will receive recognition through services that track citation counts, e.g. Scopus. If you need to cite the page number of the TSpace version (original manuscript or accepted manuscript) because you cannot access the published version, then cite the TSpace version **in addition** to the published version using the permanent URI (handle) found on the record page.



The in-gap electronic state spectrum of methylammonium lead iodide single crystal perovskites

Valerio Adinolfi¹, Mingjian Yuan¹, Riccardo Comin¹, Emmanuel S. Thibau³, Dong Shi², Makhsud Saidaminov², Pongsakorn Kanjanaboos, Damir Kopilovic¹, Sjoerd Hoogland¹, Zheng-Hong Lu³, Osman M. Bakr², Edward H. Sargent^{1*}.

¹ Department of Electrical and Computer Engineering, University of Toronto, 10 King's College Road, Toronto, Ontario M5S 3G4, Canada.

² Division of Physical Sciences and Engineering, Solar and Photovoltaics Engineering Center, King Abdullah University of Science and Technology (KAUST), Thuwal 23955-6900, Saudi Arabia

³ Department of Materials Science and Engineering, University of Toronto, 184 College Street, Toronto, Ontario M5S 3E4, Canada

Lead iodide perovskites are exceptional materials for solar energy harvesting; photovoltaic cells showing a power conversion efficiency exceeding 20% have recently been demonstrated. Impressively, these semiconductors can be deposited at room temperature using solution processing. Despite these important achievements, many fundamental properties of $\text{CH}_3\text{NH}_3\text{PbI}_3$ have remained underexplored, in part due to the nanocrystalline form of most $\text{CH}_3\text{NH}_3\text{PbI}_3$ films, a fact that obscures the inherent properties of the semiconductor in light of the major influence of grain boundaries. Recently, $\text{CH}_3\text{NH}_3\text{PbI}_3$ single crystals of millimeter size were synthesized that overcome this limitation, enabling the integrated trap state density to be reported. Here we present the first *spectrum* that details the distribution, in energy, of trap states across within the bandgap of

CH₃NH₃PbI₃ single crystals. We also report the energetic landscape of the crystal at the surface and experimentally determine mobility for both electrons and holes. This information lays a foundation for the development of accurate simulations and further progress in perovskite optoelectronic devices.

Perovskite semiconductors are one of the most striking advances in the field of thin film optoelectronic technologies, in particular for photovoltaic applications.^[1-4] In recent years, progress in perovskite materials processing has enabled rapid advances in the power conversion efficiency of perovskite-based solar cells beyond the 20% milestone.^[5,6] Impressively, this high efficiency comes in tandem with facile, inexpensive fabrication, since these materials can be solution-processed at room temperature on large-area substrates. Among perovskite materials, methylammonium lead iodide (MAPbI₃, MA=CH₃NH₃⁺) stands out as particularly promising for photovoltaics.^[7] The need to improve device performance further has spurred many researchers to investigate the fundamental properties of MAPbI₃. This semiconductor is usually synthesized in a variety of nanocrystalline forms, and its intrinsic material properties are expected to be significantly modified by extrinsic contributions from the manufacturing process, such as the effects of grain boundaries. This has driven many to investigate the electronic properties of MAPbI₃ using simulations. Density functional theory (DFT) has been widely employed to predict and evaluate critical quantities such as the effective mass for holes and electrons that give important information about the charge carrier mobility as well as the energetics of trap states.^[8-11] The number of available theoretical studies is substantial, and will benefit from direct experimental validation.

Recently, high-quality MAPbI₃ single crystals with sizes of few millimeters were synthesized;^[12] an initial characterization revealed an ultra-low density of trap states and of free carriers. Here we use these macroscopic crystals to obtain an in-depth characterization of the electronic and in-gap properties of MAPbI₃. We start with a compositional and optical investigation that confirms the quality of the material. We then experimentally determine the band diagram of the semiconductor with particular attention to its

surface properties, fundamental for the applications. The mobility and diffusion length of both electrons and holes are directly measured, as well as the concentration and type of the charge carriers. We determine the density of trap states within the electronic bandgap, identifying defect states close to both the valence and the conduction bands. This ensemble of measurements provides a more complete picture of the electronic properties of MAPbI₃. In particular, the study of the surface properties and the trap state spectrum are important for the development of solar cells and the design of light emitting diodes and light detectors.

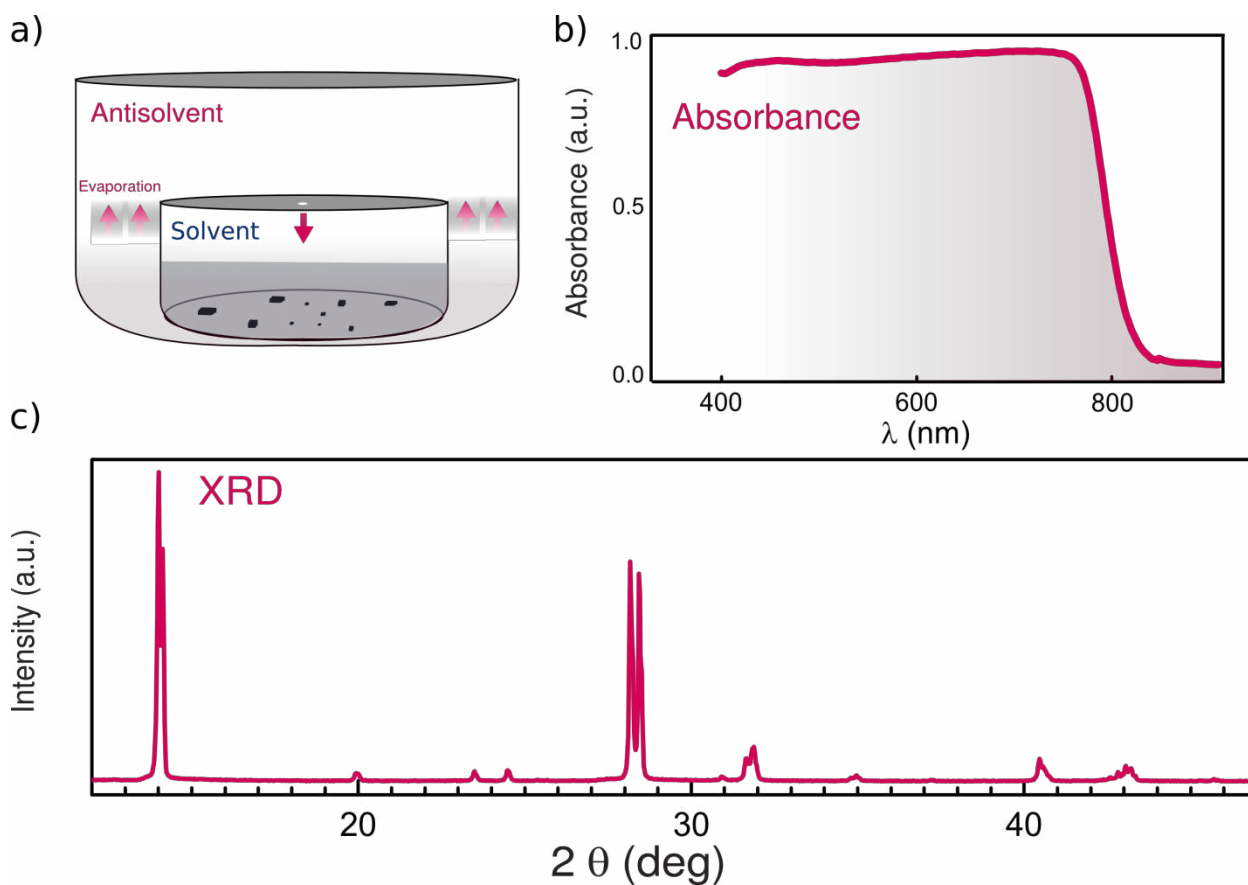


Figure 1: a) Antisolvent vapor-assisted crystallization. b) Absorbance spectrum for MAPbI₃ single crystals. c) X-ray diffraction spectroscopy diagram for MAPbI₃ crystals powder.

We synthesized MAPbI₃ single crystals using the antisolvent vapor-assisted crystallization technique.^[13] As shown in figure 1a, we prepare a solution with the precursors (MAI and PbI₂) in a small crystallizing dish. We cover the dish with aluminum foil and deposit it within a bigger container in which the antisolvent liquid resides. After we seal the outer dish, crystallization begins, with the antisolvent vapor mixing into the inner solution after it flows through a mm-sized aperture in the aluminum foil of the small crystallizing dish. The mixture between the solvent and the antisolvent sets the supersaturation conditions that promote the formation of crystalline seeds, which successively grow to the desired size.

To investigate on the purity of the crystals, we first measured the absorbance. As shown in figure 1b a steep absorption edge is located at ~810 nm, the characteristic absorption onset wavelength of MAPbI₃ single crystals.^[14–16] We further analyzed this curve to extract the optical bandgap, found to be 1.52 eV (see Supplementary Information, figure S1). To confirm further the quality of our material we performed X-ray diffraction (XRD) measurements on powders ground from single crystals. We obtained XRD with sharp Bragg reflection from tetragonal MAPbI₃, shown in figure 1c, again confirming the purity of our perovskite crystals.

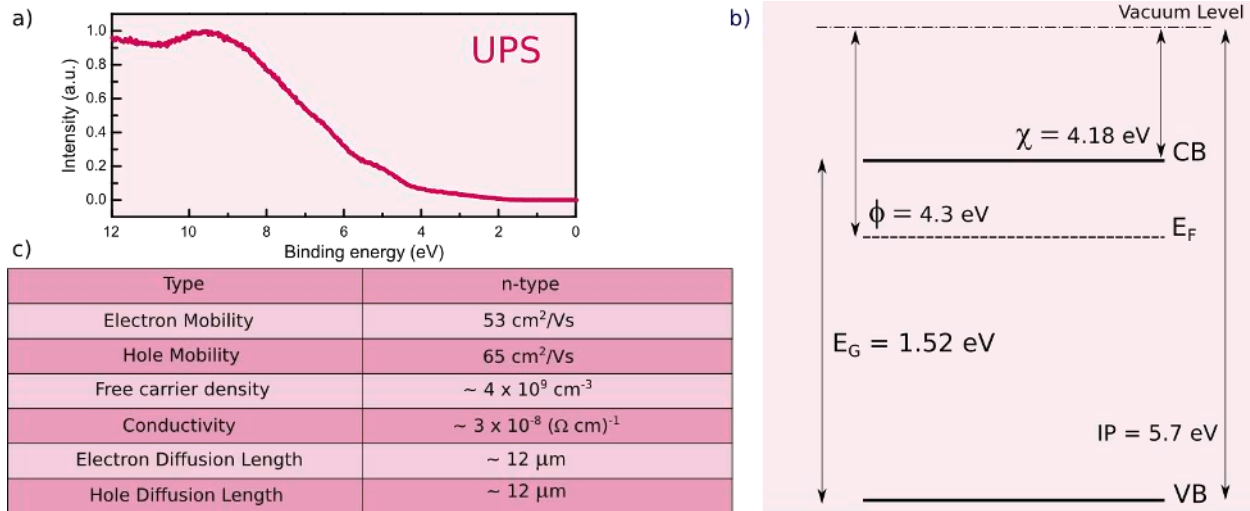


Figure 2: a) Ultraviolet photoemission spectroscopy diagram for MAPbI₃ near its surface. b) Band diagram for the near-surface of MAPbI₃ single crystals drawn according to UPS, XPS and KP measurements. c) Electronic properties of MAPbI₃ single crystals.

We therefore proceeded to the electronic characterization of the crystals. We sought to investigate, in particular, the surface properties of the crystals. To obtain the position of the valence band of MAPbI₃ relative to the vacuum level, we used X-ray (XPS, see Supplementary Information, figure S2) and ultraviolet photoemission spectroscopy (UPS, figure 2a).^[17–21] Knowing the value of the bandgap, from absorption, we depict the band diagram of the MAPbI₃ single crystals (figure 2c). The ionization potential is IP = 5.7 eV and the inferred electron affinity is $\chi = 4.18$ eV. The Fermi level at the interface is determined, using the Kelvin probe (KP) technique, to lie at 0.12 eV from the conduction band. This measurement indicates a shift of the Fermi level at the crystal surface compared to that in the bulk. The Fermi level is shifted at the surface whereas the crystal is close to an intrinsic semiconductor in the bulk^[12,16]. This shift can be attributed to the effect of trap states present on the surface of the crystals; these states have been previously identified as the cause for a fast component in the photoluminescence decay trace of MAPbI₃^[12] single crystals, and have recently been exploited to produce narrowband light detectors.^[22] The techniques used for this characterization are surface sensitive, for this reason the surface of the crystals has been accurately cleaned using appropriate wet etching right before the measurements.

To extract the relevant parameters governing electrical transport in the crystal, we performed four-points and Hall Effect measurements. Using this technique we found the free carrier concentration to be $n_f \sim 4 \times 10^9 \text{ cm}^{-3}$, in good agreement with previous reports of a near-intrinsic semiconductor.^[12] The Hall coefficient reveals that the majority carriers are electrons with a mobility of $\mu_e \sim 50 \text{ cm}^2/\text{Vs}$. Combining these two quantities, the conductivity was estimated to be $\sigma \sim 3 \times 10^{-8} \Omega^{-1}$, again in good agreement with previous findings.^[12]

The hole mobility was measured using the space charge limited current (SCLC) technique by fitting the current-voltage characteristic of the crystal in the trap free regime (Child region,^[23,24] details in Supporting Information, figure S3). We obtained a hole mobility of $\mu_h \sim 65 \text{ cm}^2/\text{Vs}$. The electron and hole mobilities are comparable, consistent with previous DFT studies that found comparable effective mass as for electrons and holes.^[8] Compared to previous reports^[12] we obtained a higher hole mobility, potentially attributable to improvements in sample preparation (see Methods).

Using the Einstein relation to extract the value of the diffusivity $D = \mu k_B T/q$, where k_B is the Boltzmann constant and q the elemental charge, and combining this quantity with the carrier lifetime τ ,^[12] (estimated from the longer component of the photoluminescence decay) we evaluate the charge carrier diffusion $L_{\text{diff}} = (D\tau)^{1/2}$ to be $L_e = L_h \sim 12 \mu\text{m}$. The results of the electronic characterization are summarized in figure 2c. These numbers reveal the potential of MAPbI₃ single crystals for optoelectronic applications, and agree well with the success of nanocrystalline thin film perovskite solar cells, since long diffusion lengths and low free carrier concentrations enable high efficiency photovoltaics. The first quantity allows for efficient extraction of photogenerated carriers over a thickness sufficient to absorb above-bandgap solar radiation; the second property further favors the collection of charge by allowing the presence of an extracting built-in electric field within the active material.

The high diffusion length and the low free carrier concentration are consequences of an extremely low density of trap states. Defects play a crucial role in the operation of solar cells and light emitting devices, as they affect the efficiency, the spectral behavior, and the operation as a function of light and electrical biases.^[25,26] Knowing the density of in-gap trap states would reveal the position in energy of these defects.

[27]

Knowing the effectiveness of the SCLC technique to study electronic properties of tri-halide perovskite single crystals, we took the view that the refinement of this approach would enable the mapping of the trap sites within the bandgap. Several studies have been conducted in the past that show how to extract the density of trap states (DOS_T) from the temperature dependence of the SCLC current-voltage characteristic in a semiconductor.^[28–30] This technique has been employed to investigate organic crystals.^[24,31,32] We explain this approach in figure 3. To probe trap states close to both valence and conduction band, we needed to prepare both hole-injecting and electron-injecting devices, respectively, since SCLC exploits unipolar transport. Hole-injecting devices were realized using $\text{MoO}_3/\text{Au}/\text{Ag}$ contacts, leveraging the deep work function of molybdenum trioxide (MoO_3).^[33,34] Electron-injecting devices were fabricated using Titanium (Ti), a shallow work function metal. The current-voltage characteristics are shown as a function of temperature for both types of devices in figure 3a and 3c. We discuss in detail the case of electron-injecting devices (figure 3b); these considerations apply symmetrically for hole-injecting devices (figure 3d).

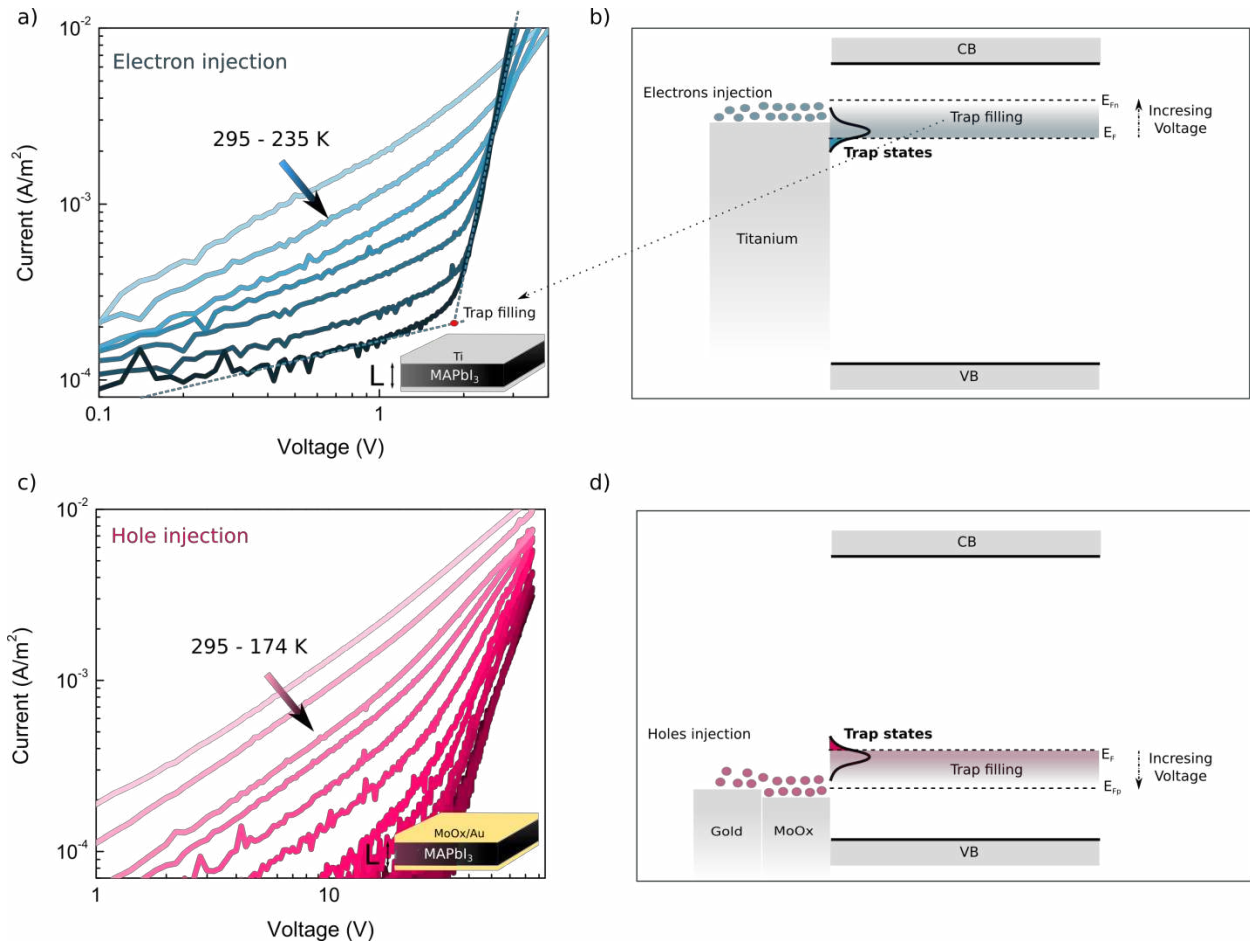


Figure 3: a) IV curve as a function of temperature for a MAPbI₃ single crystal (Area × L = (2.7×2.3)×2.0 mm) contacted using titanium (inset) to favor electron injection. b) Scheme illustrating the principles governing the SCLC method in the case of electrons injection. c) IV curve as a function of temperature for a MAPbI₃ single crystal (Area × L = (4.0×3.7)×1.3 mm) contacted using MoO₃/Au/Ag (inset) to favor hole injection. d) Scheme illustrating the principles governing the SCLC method in the case of hole injection.

Titanium forms an ohmic contact with the crystals (more details are provided in the Supplementary information, figure S5) and selectively favors electrons injection. At low applied biases the current-voltage is linear. At higher applied bias, the electron transit time becomes comparable with the relaxation time of the semiconductor. In this regime the semiconductor is replenished with electrons; and this excess of charge determines a shift of the Fermi level toward the conduction band. If trap states are present close to the Fermi level, these will be rapidly occupied by the injected electrons, leading to a transition of the current-voltage curve onto a superlinear regime ($I \propto V^m$, $m > 2$), starting at a characteristic voltage $V=V_{TFL}$. This is the

trap-filling regime. From the position of V_{TFL} , the temperature, and the derivative $\frac{\partial \ln J}{\partial \ln V}$, reconstruction of the DOS_{T} is possible.^[28]

The equations used in the model are the Ohm's law $J = e\mu n_f(x)F(x)$ and the Poisson equation $\frac{dF}{dx} = -\frac{en_s}{\epsilon}$ where $F(x)$ is the electric field as a function of the spatial coordinate x , J is the current density, ϵ is the dielectric constant, μ the mobility, n_f is the density of free carriers and n_s is the total density of carriers, both free and trapped. The latter is expressed as $n_s = \int^E h(E)f(E, E_F, T)$ where $h(E)$ is the density of trap states within the bandgap, $f(E, E_F, T)$ is the Fermi-Dirac distribution, and T the temperature of the sample. The derivative of n_s with respect to the Fermi level is^[28] $\frac{dn_s}{dE_F} = \frac{1}{k_B T} \frac{\epsilon}{qL^2} \frac{2m-1}{m^2} (1 + C)$. The parameters m and C can be extracted from the shape of the measured current-voltage characteristic (supplementary information, S5). To reconstruct the density of trap states as a function of the energy, it is also necessary to relate the voltage, V , to the energy of the traps that are filled at this specific voltage. This can be done by extracting the activation energy E_A , defined as $E_A = -\frac{d \ln J}{d(k_B T)^{-1}}$, from the temperature dependent SCLC curves at each voltage point. To extract the DOS_{T} , the expression for $\frac{dn_s}{dE_F}$ is deconvolved with respect to $\frac{df}{dE_F}$ (see Supplementary Information figure S6).

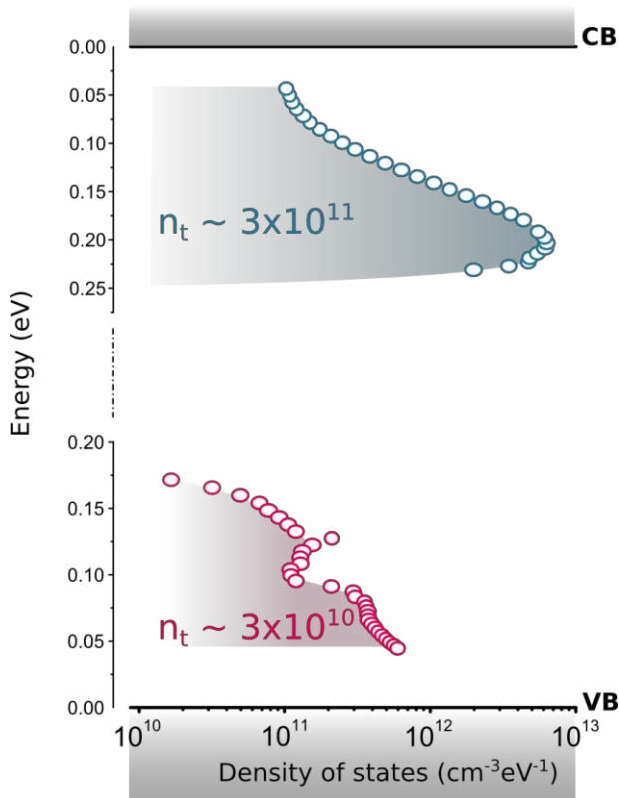


Figure 4: Density of the trap states within the bandgap so as extracted from the temperature dependent SCLC method. Trap states are identified close to the conduction and the valence bands.

After analyzing the data shown in figure 3a and 3c we were able to extract the DOS_T as in figure 4 (code validation in Supplementary Information figure S7). The analysis is consistent with previous reports: the total density of traps close to the valence band, obtained by integrating the lower part of the DOS_T with respect to energy, is confirmed to be close to $n_{VB} \sim 3 \times 10^{10} \text{ cm}^{-3}$.^[12] The same integration, performed in proximity of the conduction band region, leads to a value of $n_{CB} \sim 3 \times 10^{11} \text{ cm}^{-3}$. The DOS_T appears to be localized in energy; a defined peak is observed at $\sim 0.2 \text{ eV}$ from the conduction band, and at $\sim 0.1 \text{ eV}$ from the valence band. These findings match DFT simulations that show the presence, in very small concentrations, of trap states close to the valence and conduction bands.^[35]

In conclusion, we carried out an in-depth electronic characterization of MAPbI₃ perovskite single crystals. We experimentally confirmed a series of important hypotheses advanced in previous theoretical studies.

Furthermore, the crystals show high mobility and impressive diffusion lengths for both electrons and holes, confirming the ambipolar nature of these semiconductors.

Methods

Crystal synthesis: A mixture of PbI_2 (9.22 g, 0.02 mol) and $\text{CH}_3\text{NH}_3\text{I}$ (9.54 g, 0.06 mol) was dissolved in 40 ml of gamma-butyrolactone (GBL) to form the solution. Dichloromethane (DCM) was used as the antisolvent.

Absorbance measurements: the absorbance measurements were performed using a Jasco V-670 spectrophotometer. The sample was reduced to powder and the absorption was measured, based on the diffused reflectance, according to the established Kubelka-Munk method.

XRD measurements: XRD data were collected from MAPbI_3 single crystal powder using a Siemens D5000 Bragg-Brentano diffractometer.

UPS and XPS measurements: UPS and XPS measurements were performed in a PHI 5500 Multi-Technique system with a base pressure of $\sim 10^{-9}$ Torr. The Fermi energy was calibrated to 0 eV. The sample was set to a take-off angle of 88° and a bias of -15 V was employed to collect low-kinetic energy electrons efficiently. For XPS, monochromated Al $K\alpha$ ($h\nu = 1486.7$ eV) was used, and for UPS, non-monochromated He $I\alpha$ ($h\nu = 21.22$ eV) was used. To measure the VBM relative to the Fermi level, the onset of the valence band is linearly extrapolated to the noise level.

Kelvin Probe measurements: Kelvin probe measurements were obtained using a KPTechnology KP020 system. Both gold and aluminum were used as standard references.

IV measurements: electrical contacts were defined on parallel facets of MAPbBr_3 single crystals using thermal evaporation of $\text{MoO}_3/\text{Au}/\text{Ag}$ and e-beam evaporation of Ti for the hole-injecting and electron-injecting devices respectively. The thermal evaporator was kept in a N_2 filled glove box and was operated

at pressures below 10^{-6} Torr. Immediately before the contact deposition the crystal surfaces were cleaned using dimethylformamide. The current-voltage measurements were performed using a Keithley 2400 sourcemeter. The temperature was controlled using an Advanced Research Systems DE 202 cryostat. The samples were kept in the dark during the measurement.

References

- [1] W. Yin, J. Yang, J. Kang, Y. Yan, S.-H. Wei, *J. Mater. Chem. A* **2014**, 3, 8926.
- [2] O. Malinkiewicz, A. Yella, Y. H. Lee, G. M. Espallargas, M. Graetzel, M. K. Nazeeruddin, H. J. Bolink, *Nat. Photonics* **2013**, 8, 128.
- [3] D. Liu, T. L. Kelly, *Nat. Photonics* **2013**, 8, 133.
- [4] M. Liu, M. B. Johnston, H. J. Snaith, *Nature* **2013**, 501, 395.
- [5] M. A. Green, K. Emery, Y. Hishikawa, W. Warta, E. D. Dunlop, *Prog. Photovoltaics Res. Appl.* **2015**, 23, 1.
- [6] W. S. Yang, J. H. Noh, N. J. Jeon, Y. C. Kim, S. Ryu, J. Seo, S. I. Seok, *Science (80-.)*. **2015**, 348, 1234.
- [7] A. Marchioro, J. Teuscher, D. Friedrich, M. Kunst, R. van de Krol, T. Moehl, M. Grätzel, J.-E. Moser, *Nat. Photonics* **2014**, 8, 250.
- [8] G. Giorgi, J.-I. Fujisawa, H. Segawa, K. Yamashita, *J. Phys. Chem. Lett.* **2013**, 4, 4213.
- [9] J. Kim, S.-H. Lee, J. H. Lee, K.-H. Hong, *J. Phys. Chem. Lett.* **2014**, 5, 1312.
- [10] J. Even, L. Pedesseau, J.-M. Jancu, C. Katan, *J. Phys. Chem. Lett.* **2013**, 4, 2999.
- [11] J. M. Azpiroz, E. Mosconi, J. Bisquert, F. De Angelis, *Energy Environ. Sci.* **2015**, 8, 2118.
- [12] D. Shi, V. Adinolfi, R. Comin, M. Yuan, E. Alarousu, A. Buin, Y. Chen, S. Hoogland, A. Rothenberger, K. Katsiev, Y. Losovyj, X. Zhang, P. A. Dowben, O. F. Mohammed, E. H. Sargent, O. M. Bakr, *Science* **2015**, 347, 519.
- [13] D. J. Dixon, K. P. Johnston, *AIChE J.* **1991**, 37, 1441.
- [14] H.-S. Kim, C.-R. Lee, J.-H. Im, K.-B. Lee, T. Moehl, A. Marchioro, S.-J. Moon, R. Humphry-Baker, J.-H. Yum, J. E. Moser, M. Grätzel, N.-G. Park, *Sci. Rep.* **2012**, 2, 591.

- [15] M. I. Saidaminov, A. L. Abdelhady, B. Murali, E. Alarousu, V. M. Burlakov, W. Peng, I. Dursun, L. Wang, Y. He, G. Maculan, A. Goriely, T. Wu, O. F. Mohammed, O. M. Bakr, *Nat. Commun.* **2015**, *6*, 7586.
- [16] Q. Dong, Y. Fang, Y. Shao, P. Mulligan, J. Qiu, L. Cao, J. Huang, *Science (80)* **2015**, *347*, 967.
- [17] J. S. Kim, B. Lägél, E. Moons, N. Johansson, I. D. Baikie, W. R. Salaneck, R. H. Friend, F. Cacialli, *Synth. Met.* **2000**, *111-112*, 311.
- [18] H. Baumgärtner, H. D. Liess, *Rev. Sci. Instrum.* **1988**, *59*, 802.
- [19] A. Pfau, K. D. Schierbaum, *Surf. Sci.* **1994**, *321*, 71.
- [20] P. Oelhafen, M. Liard, H.-J. Güntherodt, K. Berresheim, H. D. Polaschegg, *Solid State Commun.* **1979**, *30*, 641.
- [21] L. Ley, R. A. Pollak, F. R. McFeely, S. P. Kowalczyk, D. A. Shirley, *Phys. Rev. B* **1974**, *9*, 600.
- [22] Y. Fang, Q. Dong, Y. Shao, Y. Yuan, J. Huang, *Nat. Photonics* **2015**, *9*, 679.
- [23] A. Rose, *Phys. Rev.* **1955**, *97*, 1538.
- [24] P. Mark, W. Helfrich, *J. Appl. Phys.* **1962**, *33*, 205.
- [25] M. M. Mandoc, F. B. Kooistra, J. C. Hummelen, B. de Boer, P. W. M. Blom, *Appl. Phys. Lett.* **2007**, *91*, 263505.
- [26] M. Bailes, P. J. Cameron, K. Lobato, L. M. Peter, *J. Phys. Chem. B* **2005**, *109*, 15429.
- [27] A. H. Ip, S. M. Thon, S. Hoogland, O. Voznyy, D. Zhitomirsky, R. Debnath, L. Levina, L. R. Rollny, G. H. Carey, A. Fischer, K. W. Kemp, I. J. Kramer, Z. Ning, A. J. Labelle, K. W. Chou, A. Amassian, E. H. Sargent, *Nat. Nanotechnol.* **2012**, *7*, 577.
- [28] F. Schauer, R. Novotny, S. Nešpůrek, *J. Appl. Phys.* **1997**, *81*, 1244.
- [29] S. Nespurek, E. A. Silinsh, *Phys. Status Solidi* **1976**, *34*, 747.
- [30] J. Dacuña, A. Salleo, *Phys. Rev. B - Condens. Matter Mater. Phys.* **2011**, *84*.
- [31] C. Krellner, S. Haas, C. Goldmann, K. P. Pernstich, D. J. Gundlach, B. Batlogg, *Phys. Rev. B - Condens. Matter Mater. Phys.* **2007**, *75*.
- [32] M. A. Lampert, A. Rose, R. W. Smith, *J. Phys. Chem. Solids* **1959**, *8*, 464.
- [33] H. Lee, S. W. Cho, K. Han, P. E. Jeon, C.-N. Whang, K. Jeong, K. Cho, Y. Yi, *Appl. Phys. Lett.* **2008**, *93*, 043308.
- [34] W.-J. Shin, J.-Y. Lee, J. C. Kim, T.-H. Yoon, T.-S. Kim, O.-K. Song, *Org. Electron.* **2008**, *9*, 333.

- [35] A. Buin, P. Pietsch, J. Xu, O. Voznyy, A. H. Ip, R. Comin, E. H. Sargent, *Nano Lett.* **2014**, *14*, 6281.

Acknowledgments

We thank Prof. Gennaro (Rino) Conte for the valuable discussions. We thank Damir Kopilovic for the technical assistance. This publication is based in part on work supported by Award KUS-11-009-21 made by King Abdullah University of Science and Technology (KAUST), by the Ontario Research Fund - Research Excellence Program, and by the Natural Sciences and Engineering Research Council (NSERC) of Canada.